

Linearity and sensitivity of MIS position sensitive detectors

H. ÁGUAS*, L. PEREIRA, D. COSTA, E. FORTUNATO, R. MARTINS

Departamento de Ciência dos Materiais/CENIMAT, Faculdade de Ciências e Tecnologia, Universidade Nova de Lisboa, CEMOP/UNINOVA, Campus da Caparica, 2829-516 Caparica, Portugal

E-mail: hma@fct.unl.pt

The linearity and sensitivity of linear Position Sensitive Detectors (PSD) are the two principal characteristics of sensors to be optimised in sensor fabrication. This work presents several efforts made to understand the internal and external parameters that influence the linearity and sensitivity of Metal Insulator Semiconductor (MIS) linear PSD with an active length of 6 cm. The use of long sensitive areas allows the PSD to achieve greater resolution without the need of a highly accurate light spot integration mechanism. The PSD is built in a multi-layered structure consisting of Cr/a-Si:H (n^+ doped)/a-Si:H (intrinsic)/SiO_x (passivation layer)/Au, where the active a-Si:H layers were deposited by Modified Triode Plasma Enhanced Chemical Vapour Deposition (MTPECVD), which allows the deposition of good electronic grade material with a low ($\approx 1 \times 10^{15} \text{ cm}^{-3}$) defect density inferred by CPM. The sensor linearity and sensitivity shows dependence on the sensor width to length ratio, SiO_x layer and on the value of the load resistance. Sensitivities of more than 30 mV/cm were achieved with linearity near 99%. Besides that, this type of MIS structure allows an improved spectral response in the near-UV region and has its maximum response at 540 nm. © 2005 Springer Science + Business Media, Inc.

1. Introduction

The subject of position sensitive detectors (PSD) has been the concern of several publications in the past two decades [1–3]. The privileged active material in the PSD research has been the hydrogenated amorphous silicon (a-Si:H) due to its low cost and the easiness of depositing layers in large areas. The Metal–Insulator–Semiconductor (MIS) type of structure has been used in the PSD fabrication since the first works by Arimoto *et al.* [4] that reported a sensor with a length of 1 cm length. The main goals in the PSD research have been the increase in sensor length, sensitivity and resolution of the sensors. Just to state a few examples: a sensor with a length of 4 cm was produced using a p-i-n structure [2]; a multilayer system (MLS) of a-Si:H/Ti has been used to fabricate sensors with 1 cm of length and sensitivity of 1 mV/cm [5]; a sensor consisting of ITO deposited in crystalline *p* doped silicon was proposed [6]. This sensor, which had an absolute excellent linearity, had a length of 0.4 cm and a sensitivity of 20 mV/cm.

In this work we studied a 1 dimensional PSD sensor based in a-Si:H/oxide/Au structure, with an active length of 6 cm and presenting good sensitivity in the voltage measurement mode [2]. The data achieved showed to be highly dependent on the SiO_x passivation layer. Besides that, we investigate the role of the load

resistance (R_L) and sensor geometry in the sensitivity and linearity.

2. Experimental

The sensor structure consists of 5 layers deposited on a 2 mm glass substrate: Cr (300 nm)/a-Si:H [n^+ doped] (40 nm)/a-Si:H [intrinsic] (550 nm)/SiO_x (1.5 nm)/Au (7 nm). The metals were deposited by evaporation in an Electron Gun system. The a-Si:H was deposited by plasma enhanced chemical vapour deposition (PECVD) of silane, and the SiO_x layer was grown prior to the Au metallization by heating the sample for 3 h at 160°C. This process fastens the formation of the a-Si:H native oxide. Alternatively we tested a sensor that developed an overly insulating oxide SiO_x layer by reaction with the Au layer [7].

The sensors were characterized by linearity measurements performed by scanning the sensor with a green laser of 532 nm of wavelength and a power of 5 mW (spot size of about 1 mm).

Fig. 1 shows a scheme of the sensor where the width (W) and the length (L) of the active region are indicated. It is also shown the external connections, where the load resistances (R_L) and the voltmeter (V) are indicated.

In order to determine which parameters influence the sensitivity and linearity of the sensor, linearity

*Author to whom all correspondence should be addressed.

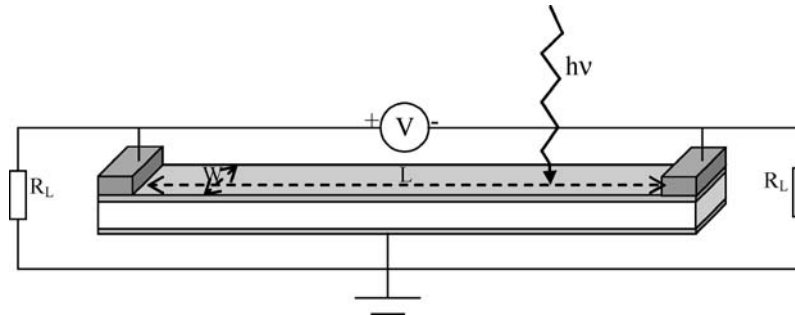


Figure 1 Schematic of the sensor structure, dimensions width (W) and length (L) and external connections.

measurements were performed using values of R_L from ∞ to 100Ω in sensors with different W/L ratio geometries, by varying the sensor width from 7 to 1 mm and keeping the length constant. Besides that, it is shown that the sensor sensitivity and linearity can be improved if an external bias voltage is applied to the sensor, although this improvement is most effective if applied to a MIS sensor with an excessive thickness of oxide, 3.5 nm in the case studied, which caused a bad sensor performance without applied bias.

The linearity error σ was determined by the relation: $\sigma = 2S/F$ [2], where S is standard deviation of the measure and F is the full scale of the measure. Acceptable devices have linearity errors less than 15% [8].

3. Results

The MIS structure studied has the maximum of the spectral response located in the green region of the light spectrum, which means that the sensor will have a better response if illuminated with a green laser. Fig. 2 shows the spectral response of the MIS diode structure used to fabricate the diode. The maximum of the response is located at 540 nm and the laser beam used has a wavelength of 532 nm, which is very close to the maximum of the sensor. Besides that, Fig. 2 also shows that the sensor has a good response in the near-UV region, meaning that it might be used there.

One of the most important characteristics that the MIS structure must possess is a high light to dark reverse current ratio (I_{ph}/I_d). This result comes from the model that describes the photolateral effect [9], which

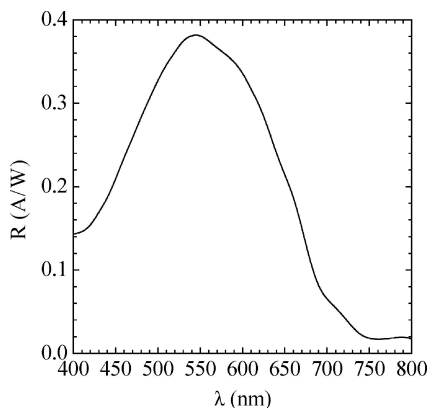


Figure 2 Spectral response of the MIS structure used to build the sensors. The maximum of the response is located at 540 nm.

establishes the fall off parameter (α) that depends on the characteristics of the sensitive and resistive layers of the sensor and is basically a product of the sheet resistance of the resistive layer by the transversal conductivity of the structure. For a MIS structure, the absence of the semiconductive layer (typically an a-Si:H p layer) between the photosensitive layer (intrinsic a-Si:H) and the resistive layer (Au), simplifies α in to [9]:

$$\alpha = \rho_s \sigma_0 \frac{2a}{W} \frac{2a}{W_r} \tag{1}$$

where ρ_s is the sheet resistance of the resistive layer, σ_0 the conductivity of the photosensitive layer, W the thickness of the photoconductive layer, W_r the thickness of the resistive layer and a the radius of the light spot in the surface. These parameters for the MIS sensors are typically: $\rho_s = 5 \Omega/\square$; $W_r = 70 \text{ \AA}$; $W = 6000 \text{ \AA}$; $a = 0.5 \text{ mm}$; $\sigma_0 = 10^{-11} (\Omega\text{cm})^{-1}$, which gives $\alpha = 0.012$. This value is much lower than 1, the limit situation below which linearity appears, so it is expected the sensor to be quite linear if the uniformity of the layers are achieved during the fabrication process of the sensor.

Fig. 3 shows the equivalent electric circuit of the sensor. The generator in the middle represents the generated electron—hole charges in the place where the laser beam impinges the sensor. The left and right sides of the circuit corresponds to the areas of the sensor at left and right of the laser beam position, which are diodes that establish the photo-generated voltage (V_G). The parallel resistance (R_P) represents the recombination paths along the sensor length. The series resistance (R_S) represents the path that the charges have to travel

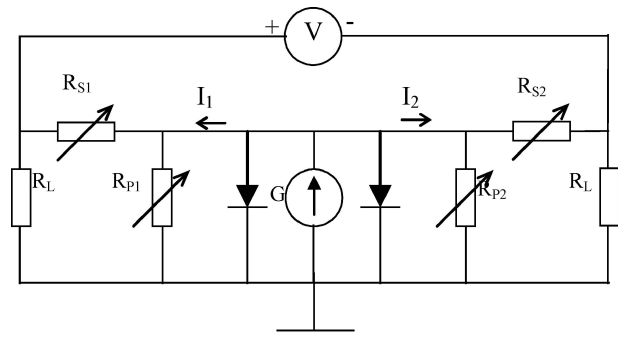


Figure 3 Equivalent electric circuit of the sensor with external connections to the load resistances (R_L) and voltmeter.

to reach the device contacts in the extremes of the sensor. In each extreme there should be connected a R_L , while the voltmeter is connected between the two contacts of the sensor in the extremes. A more accurate model should have included a capacitor in parallel with R_P , which was omitted since it is not important to the static analysis of the circuit.

It is important to note that $R_{S1} + R_{S2}$ correspond to the total resistance of the sensor Au top contact, measured between extremes. This means that when R_{S1} decreases by ΔR , R_{S2} increases by ΔR .

From the circuit we have that:

$$V = I_{RS1}R_{S1} - I_{RS2}R_{S2} \quad (2)$$

Since the input resistance of the electrometer voltmeter resistance is much larger than R_L (typically 10 to 100 M Ω), we can say that $I_{RS} = I_{RL}$, in each branch of the circuit.

Also, if we choose R_L so that:

$$(R_L + R_{S1}) \ll R_P \quad (3)$$

we can neglect the current that passes through R_P and so Equation 2 becomes:

$$V = I_1R_{S1} - I_2R_{S2} \quad (4)$$

Finally, if R_L is chosen so be larger than the overall top contact resistance ($R_{S1} + R_{S2}$), we can say that $I_1 \approx I_2 \approx I$ and Equation 4 simplifies to de ideal relation:

$$V = I(R_{S1} - R_{S2}) \quad (5)$$

which corresponds to a linear dependence of the voltage measured with the laser beam position.

So, the best linearity should be obtained when the value of R_L is correctly chosen. In the case of the sensors studied in this work, R_S is very low, since the Au is highly conductive, typically in the range of 50 to 500 Ω , depending on the width of the sensor, while R_P is typically in range of the tens of k Ω . This means that the ideal value of R_L should be chosen to be between the values of R_S and R_P .

Fig. 4a shows the linearity measurements performed on a sensor placed in dark conditions, i.e. it is just illuminated locally by the laser spot. The curves are linear over the total 6 cm range of the sensor. It is observed that the sensitivity of the sensor is maximized for an R_L value of 1 k Ω . For values larger (10 k Ω) or lower (100 Ω) than 1 k Ω the sensitivity decreases. The values of the sensitivity are shown in Table I, which also indicates the linearity error of the measurements. These data show that the sensor linearity is better for the condition of $R_L = 1$ k Ω , being much worse when no R_L is connected, which corresponds to the $R_L = \infty$ condition. This result agrees with the proposed model for the sensor measurement with one voltmeter. This value of R_L is between the typical values of R_P and R_S of the sensor, so it agrees well with the theory.

Fig. 4(b) shows the same linearity measurements performed for Fig. 4a, but now with the sensor exposed to diffuse light from environment. Table I presents the sensitivity and linearity error of these measurements. It is observed that the sensitivity of the sensor in light environment conditions is always higher, specially when $R_L = \infty$, and also that for this value of R_L the linearity is better. This behaviour could be ascribed to the fact that even under low illumination conditions, the structure is depleted, and so, the output resistance of the device increases. Besides that, the diffused light causes a uniform charge generation that opposes the charge recombination that occurs along the sensor area, when the laser spot illuminates the sensor in a single point. This situation is evidenced when $R_L = \infty$ since in this case, the losses though R_P dominates and the sensitivity is low. The uniform illumination of the sensor with diffused light allows then a better sensitivity and linearity when high values of R_L are used, than when the sensor is in the dark. On the other hand, with illumination, for an R_L of 1 k Ω and 100 Ω the linearity error is slightly larger since in these conditions the sensor sensitivity is high and it is difficult to guarantee that the charge generation is uniform in the entire sensor due to the environment light.

Fig. 5 shows the linearity measurements performed on sensors with different W/L ratios. Fig. 6 presents

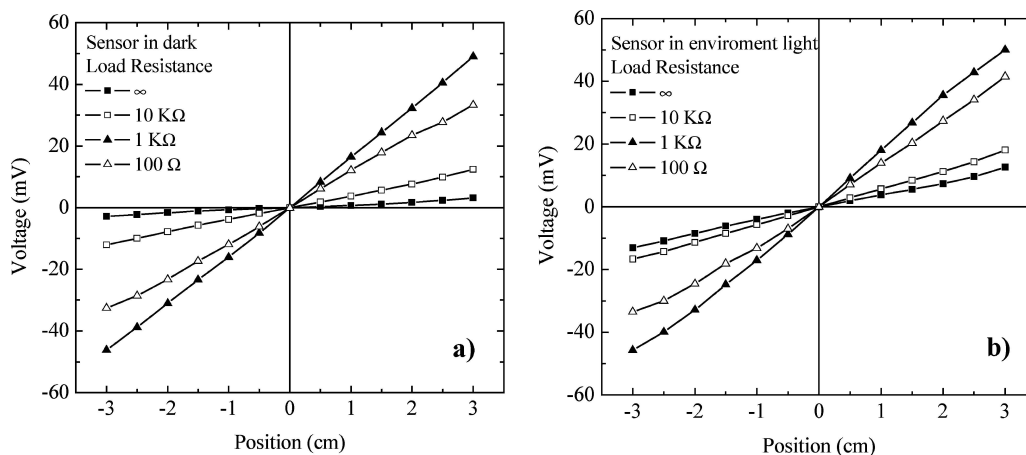


Figure 4 Voltage measured across the sensor as function of the laser beam position for different load resistances. (a) Measures performed in dark environment conditions. (b) Measures performed under diffuse light environment conditions.

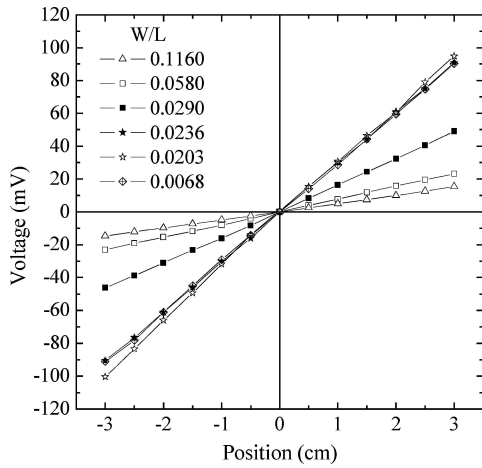


Figure 5 Differential voltage measurement versus laser beam position, for different sensor width (W) to length (L) ratios.

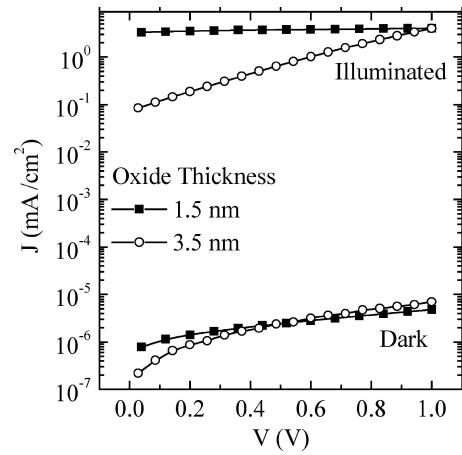


Figure 7 Influence of the oxide thickness on the photocurrent and dark currents of the MIS structure with reverse polarization.

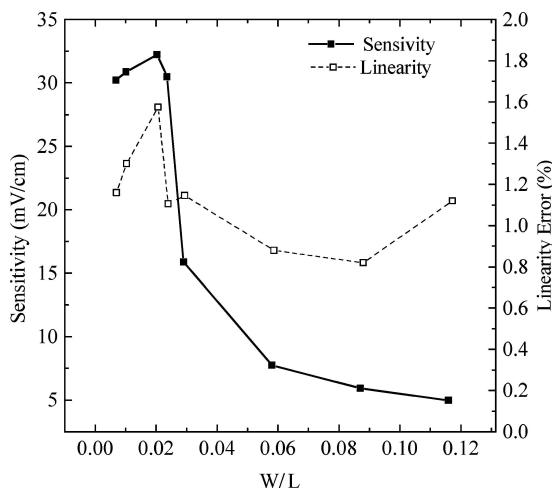


Figure 6 Sensitivity and linearity error as function of the sensor width (W) to length (L) ratio.

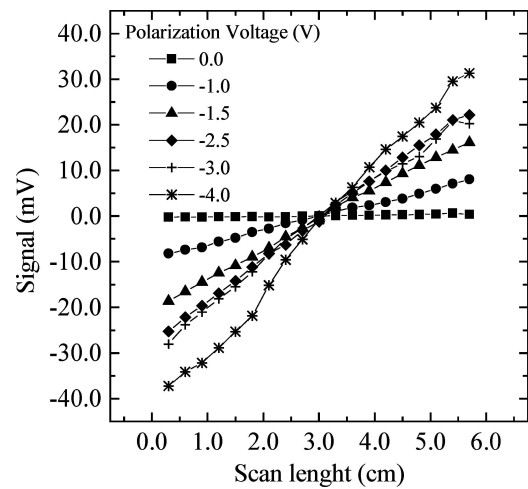


Figure 8 Linearity measurements performed on a MIS sensor with an insulating oxide with different applied bias voltages.

the sensitivity and linearity error of the different sensor geometries. R_L is $1\text{ k}\Omega$ in all measurements that were performed in the dark. It is observed that the sensitivity increases with the decrease of the W/L ratio, up to $W/L = 0.02$, where it saturates. On the other hand, in spite of the increase in sensitivity, the linearity error is not improved and stays near to 1.2%, where the lower values are obtained for W/L between 0.06 and 0.09. These results show that the decrease in W/L results in an increase of both R_S and R_P , resulting in the increase of the sensitivity. In spite of this, the linearity is relatively independent of the sensor geometry, which means that the R_S and R_P characteristics affect mostly the sensitivity, while that the linearity is more dependent on R_L .

The influence of applying a polarization voltage to deplete the junction is much more significant in the case of sensors where the thin insulation layer of SiO_x is overly insulating, due to excess of thickness, in a way that the photocurrent is strongly reduced under no applied bias voltage conditions as it is shown in Fig. 7. In this type of sensors if a bias is not applied, the sensitivity is quite low as the data in Figs 8 and 9 show, where a negative bias was applied to the sensor through

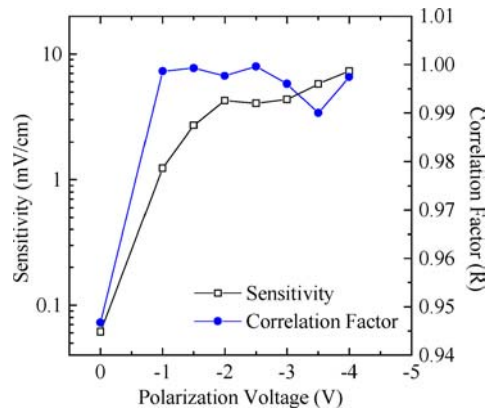


Figure 9 Sensitivity and correlation factor of the sensor with insulating oxide as function of the applied bias.

a load resistance of $1\text{ k}\Omega$. This data show that the application of a polarization bias to the sensor, increases its sensitivity by increasing the ratio I_{ph}/I_d , besides increasing the linearity and the correlation factor of the data points shown. In spite of this, the data also show that an increase of V_{bias} above 2.5 V causes the appearance of distortion in the curves, which decreases the linearity.

4. Conclusions

The MIS sensor structure proposed in this work presents a good linearity over a wide length of 6 cm. It is also shown that the use of the adequate R_L is important in improving the linearity of measurements performed with a single voltmeter. The results also show that this type of sensor works well in light environment conditions, with an increased sensitivity and only a small increase of the linearity error. Under dark conditions the linearity error decreases and the ideal value of load resistance is of the order of 1 k Ω .

The sensor geometry used is also important in determining the sensor sensitivity, which increases when low W/L ratios are used. A small polarization voltage should be used to increase the sensitivity and linearity of MIS sensors with low I_{ph} due to an overly insulating oxide layer.

Acknowledgements

This work was performed in the frame of the Prime program of the Portuguese Ministry of Economy (SENSIT project), POE, action B3, medida 3.1, ref. 03/00197. Besides that the work was also supported by "Fundação

para a Ciência e a Tecnologia" through pluriannual contract with CENIMAT.

References

1. S. ARIMOTO, H. YAMAMOTO, H. OHNO and H. HASEGAWA, *J. Appl. Phys.* **57** (1985) 4778.
2. E. FORTUNATO and R. MARTINS, *Rev. Sci. Instrum.* **67** (1996) 2702.
3. J. HENRY and J. LIVINGSTONE, *J. Opt. A: Pure Appl. Opt.* **4** (2002) 1.
4. S. ARIMOTO, H. YAMAMOTO, H. OHNO and H. HASEGAWA, in Extended Abstracts of the 15th Conference on Solid State Devices and Materials, Tokyo (1983) p. 197.
5. A. N. PANCKOW, J. BLASING and T.P. DRUSED AU, *J. Non-Cryst. Solids* **164-166** (1993) 845.
6. S.S. GERGOGIEV, D. SUEVA and N. NEDEV, *J. Phys. Condens. Matter.* **9** (1997) 4995.
7. H. ÁGUAS, L. PEREIRA, I. FERREIRA, A. R. RAMOS, A. S. VIANA, J. ANDREU, P. VILARINHO, E. FORTUNATO and R. MARTINS, "Effect of Annealing on Gold Rectifying Contacts in Amorphous Silicon," Materials Science Forum (2004) in press.
8. E. FORTUNATO, G. LAVAREDA, R. MARTINS, F. SOARES and L. FERNANDES, *Sens. & Actuat. A* **51** (1996) 135.
9. E. FORTUNATO and R. MARTINS, *Solid State Phenomena* **44-46** (1995) 883.